Proceedings of the 20th International Conference on Soil Mechanics and Geotechnical Engineering– Rahman and Jaksa (Eds)

Site-specific probabilistic seismic hazard assessment for Nuku'alofa, Kingdom of Tonga

Évaluation probabiliste du risque sismique spécifique au site pour Nuku'alofa, Royaume des Tonga

Carolina Sigarán-Loría & Casper Gies
Royal HaskoningDHV, Nijmegen, The Netherlands

Stamatina Marinatou
Royal HaskoningDHV, Rightwell House, Bretton, Peterborough, United Kingdom

ABSTRACT: A site-specific probabilistic seismic hazard assessment (PSHA) was performed to prescribe ground motion parameters for seismic-resistant design of Queen Salote International Wharf (QSIW) Upgrade Project. The study was important since only global and regional hazard models are available for the region, showing large discrepancies. Undertaking this work was a low-regret measure to address the extreme risk the region's high seismicity poses to existing and new developments, as has been demonstrated by recent strong earthquakes which caused significant infrastructure damage, displacement or loss of life in the island. The site-specific PSHA entails the latest knowledge of the seismotectonic setting of the region. A comprehensive catalog (declustered and complete for events of Mw≥ 5) was created from recognized sources with historical and instrumental seismicity. The PSHA followed a standard logic-tree approach considering epistemic uncertainties for the ground motion parameter predictions in two branches for active crustal regions and subduction zones. The hazard was assessed for various scenarios (2%, 5%, 10% and 50% probabilities of exceedance in 50 years) and two site conditions, corresponding to the local bedrock and native ground profile present at the site, characterized with mean shear wave velocity profiles from the upper 30 m (Vs30) of 760m/s and Vs30=400m/s respectively, as measured by downhole tests. The native ground profile was re-evaluated at a later stage with further ground investigation data (SPTs) and the associated site class interpreted. Design elastic spectra were derived following prescriptive values from New Zealand and U.S. Standards and compared with the site-specific PSHA.

RÉSUMÉ: Une évaluation probabiliste des risques sismiques (PSHA) propre au site a été réalisée pour prescrire les paramètres de mouvement du sol pour la conception antisismique du projet de mise à niveau du quai international Queen Salote (QSIW). L'étude était importante car seuls des modèles de risques mondiaux et régionaux sont disponibles pour la région, montrant des écarts importants. Entreprendre ce travail était une mesure à faible regret pour faire face au risque extrême que la forte sismicité de la région pose aux développements existants et nouveaux, comme l'ont démontré les récents tremblements de terre violents qui ont causé des dommages importants aux infrastructures, des déplacements ou des pertes de vie dans l'île. Le PSHA spécifique au site implique les dernières connaissances sur le contexte sismotectonique de la région. Un catalogue complet (pour les événements de Mw ≥ 5) a été créé à partir de sources reconnues avec une sismicité historique et instrumentale. Le PSHA a suivi une approche d''logic tree' tenant compte des incertitudes épistémiques pour les prédictions des paramètres de mouvement du sol pour les régions crustales actives et les zones de subduction. Le danger a été évalué pour différents scénarios (probabilités de dépassement de 2%, 5%, 10% et 50% en 50 ans) et deux conditions du site, correspondant au substrat rocheux local et au profil du sol natif présents sur le site, caractérisés par une onde de cisaillement moyenne profils de vitesse à partir des 30 m supérieurs (Vs30) de 760 m / s et Vs30 = 400 m / s respectivement, mesurés par des essais en fond de puits. Le profil du sol natif a été réévalué à un stade ultérieur avec des données d'enquête au sol supplémentaires (SPT) et la classe de site associée interprétée. Les spectres élastiques de conception ont été dérivés en suivant les valeurs prescriptives des normes néo-zélandaises et américaines et comparés au PSHA spécifique au site.

KEYWORDS: Probabilistic seismic hazard; site-specific hazard; seismic resilient design; Tonga.

1 INTRODUCTION

Tongatapu is in an area of high seismicity, next to one of the most active subduction zones in the world. Despite the large seismic risk from the region, there is scarce and inconsistent seismic hazard literature. Besides the global hazard maps available (e.g. GEM by Pagani et al., 2018 and SED, 2016), there are few regional hazard studies covering Tongatapu from Rong et al., 2010, 2012 and Petersen et al., 2012. Rong's work was part of a regional World Bank project to set country-specific seismic risk profiles, while Petersen's aim was to consider implementing it within the International Building Code (2012-edition).

This site-specific probabilistic seismic hazard assessment (PSHA) is part of the feasibility and disaster and climate resilient upgrade works of Queen Salote International Wharf (QSIW), funded by the Asian Development Bank (ADB).

2 SEISMOTECTONIC AND GEOLOGICAL SETTING

The Tongatapu island is situated on the Tonga Ridge, approximatively 150 km west from the Tonga-Kermadec megathrust subduction boundary with the Pacific Plate and east of the Lau back-arc basin (Figure 1). This region moves independently from the Australian and Pacific plates and is subdivided into several smaller plates like the Tonga, Kermadec and Niuafo'ou plates. Tongatapu sits on the Tonga microplate which actively rifts apart from the Australian and Niuafo'ou plates on the western edge. On the eastern end the Pacific plate subducts beneath the Tonga microplate. The northern edge of the microplate is separated from the Pacific plate by the westward curvature of the Tonga trench changing into a transform Fiji fracture zone and the extinct subduction of the Vitiaz trench (Figure 1) (Bevis et al., 1995).

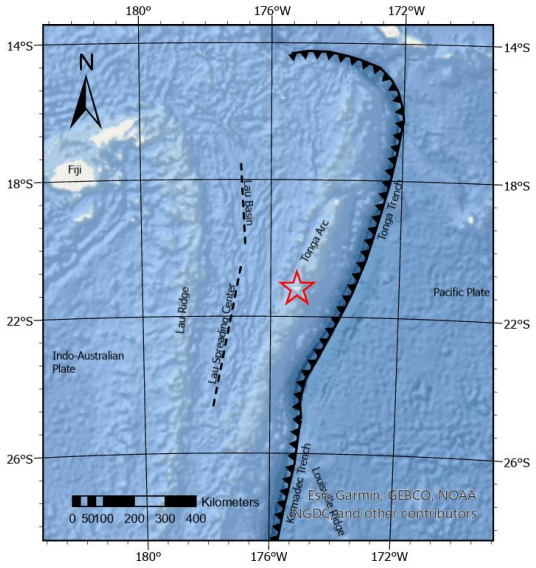

Figure 1. Regional tectonic map (after Contreras-Reyes et al., 2011). Red star indicates Tongatapu.

The regional tectonic evolution from Mid-Late Eocene to present day is illustrated in Figure 2. A former island arc chain from the Mid-Late Eocene (Figure 2a) was subdivided by back-arc spreading during the Oligocene (Figure 2b). During the Late Miocene the northern New Hebrides arc reversed and started separating the previous island arc chain (Figure 2c). Tectonism increased in the southern Fiji-Lau-Tonga arc causing doming, E-W normal faulting (orthogonal to the N-S orientated Tonga trench) and westward tilting associated with intrusive activity. From Late Pliocene to Quaternary a second back-arc spreading phase at the Lau basin drifted the Lau and Tonga arc apart to their current locations (Figure 2d) (Austin et al., 1989).

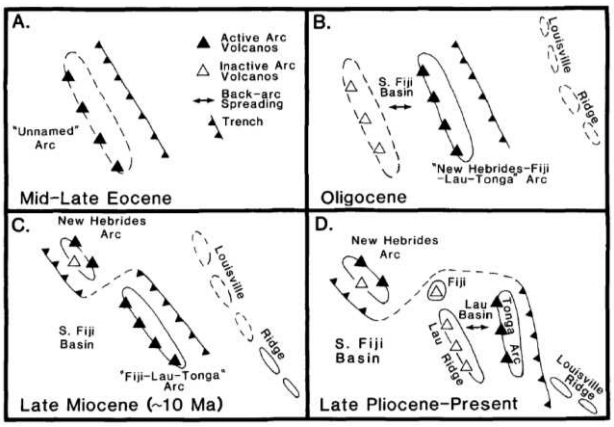

Figure 2. Schematic tectonic history of the Tonga region. Dashed lines indicate inferred morphologic features (after Austin et al., 1989).

The geology from Tongatapu island is typical for the larger Tonga arc system. Middle Eocene volcanic rocks are the oldest rocks found, forming an igneous geological basement in the region. These volcanic rocks comprise agglomerates, lava flows, tuffs and dykes. Above the volcanic basement, is a roughly 2000 m thick sedimentary sequence of volcaniclastic turbidites and hemipelagic sediments from the upper Eocene to upper Miocene. This sequence is interrupted by three geological unconformities from early Oligocene, early Miocene and early Pliocene ages. These unconformities show evidence of multiple reworking and are intercalated with various neritic limestone beds (Austin et al., 1989). Above the youngest unconformity there is a Pliocene to Holocene foraminiferal and coral limestone. This formation has a thickness of 250 m at the southern end of Tongatapu, decreasing northwards to near 150 m at the northern edge, by Nuku'alofa (Spennemann, 1997).

3 SEISMICITY

An earthquake catalog was constructed covering historical and instrumental periods, by compiling global and regional catalogs from the following recognized institutions: i. ISC-GEM (GEM, 2019), ii. ISC (ISC, 2019), iii. Ministry of Natural Resources of Tonga (MNRT, 2019), iv. USGS (USGS, 2019) and v. Geoscience Australia (GA, 2019). The catalogs were retrieved for a region extending 350 km from QSIW, comprising earthquakes from 1906 to 2019. Duplicate events were removed considering the above outlined prevalence order. The MNRT catalog was obtained by written communications during November 2019. This catalog is a data join from USGS and Oceania Regional Seismic Network (ORSET). The ISC-GEM was set as primary source of data due to the consistent manner of event processing to generate a homogeneous catalog with reviewed magnitudes (Di Giacomo et al. 2015, 2018) and improved depth and location estimates (Bondar et al., 2015 in ISC-GEM, 2019).

When merging the catalogs, duplicate entries and events with unknown depths or magnitudes were removed. The merged catalog was subsequently homogenized in magnitude by converting local (M_L), standard broadband (m_B), body-wave (m_b) and surface-wave (M_s) magnitudes to moment magnitude (M_w). For this process, the equations proposed by McGuire (2004), Bormann and Saul (2008) and Di Giacomo et al. (2015) were used. To comply with the assumption of statistical independence in both time and space, the catalog was declustered using the methodology of Gardner and Knopoff (1974). For the available dataset only events with $M_w \leq 5.5$ were affected. Under the principle of stationary seismicity, the catalog completeness was reviewed for different magnitude bins. Events with $M_w > 8.0$ were not removed and the final catalog was considered complete for events with $M_w \geq 5.0$ that have occurred since 1974, comprising in total 2978 events (Figure 3).

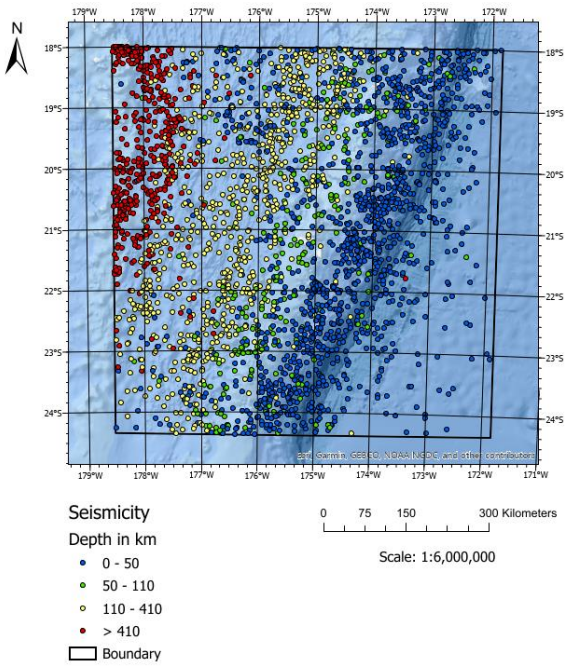

Figure 3. Final earthquake catalog with $M_w \geq 5$ from 1919 to 2019 used for this assessment grouped per hypocentral depth.

4 SEISMIC SOURCE MODEL

The source model comprises eleven seismic sources, seven associated to active crustal regions (ACR), up to 50 km depth and four to subduction zones (SZ), extending down to 700 km (Figure 4). Some of the source zone boundaries are following the obvious tectonic features that are determined by the outline of the Pacific Plate (2) and the Fonualei discontinuity (5), while the Lau Basin (4) and Tonga Interplate-A/B (6/9) are based on the seismicity distribution in space and depth in combination with the boundaries used by Rong et al. (2010, 2012). Despite that the seismicity from the Australian Plate is low, it is modelled as ACR given the scarce information from the region and to remain aligned with the assumption made by the earlier regional studies from both Rong et al. (2010, 2012) and Petersen (2012).

The Tonga Interplate (9, 10) and Tonga Ridge (6, 11) are divided in two parts (A and B), after the observed decrease in seismicity northwards. Similarly, the Intraslab is divided in two depth zones: Intraslab Deep (8) and Intraslab Intermediate (7) based on cross sections of the seismicity (example in Figure 5). There is an apparent overlap between Zones 7 and 8, due to their projection to surface from the 3D features. The zoning from this assessment is similar to Rong et al. (2010, 2012), but this work enhanced the level of spatial detail.

To prevent double counting of seismicity and constrain epistemic uncertainties in the interpretation, the interplate zones are conservatively modelled as 3D area sources with reverse source rupture model, implementing the Magnitude-rupture area relation from Wells and Coppersmith (1994). For the remaining source zones a generic source rupture model was used, also from Wells and Coppersmith (1994). In R-CRISIS the source rupture is assumed circular for area and smoothed seismicity (gridded) sources (R-CRISIS, 2019). The shortest distance from the interplate to Nuku'alofa Port is approximately 40 km.

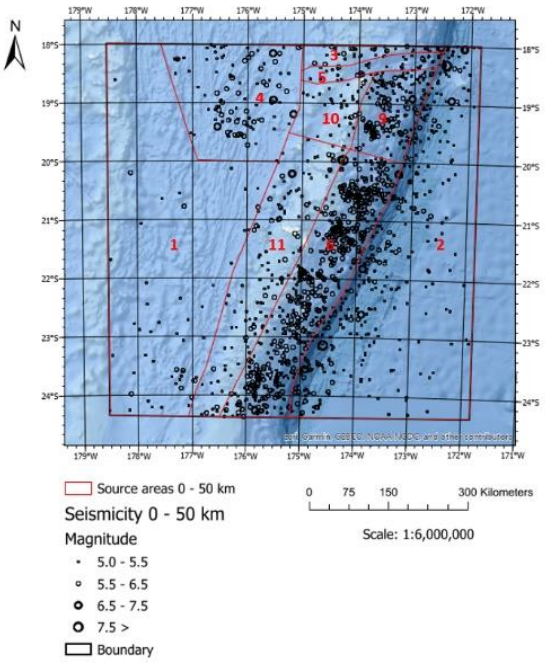

a)

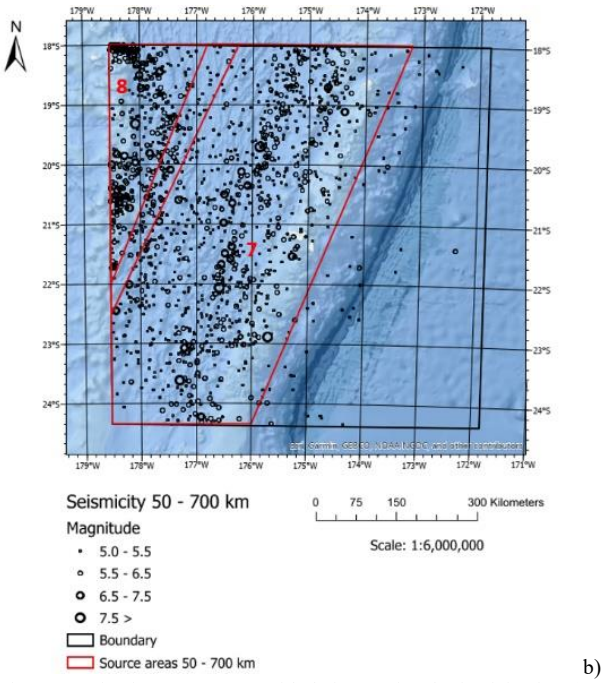

b)

Figure 4. Seismic source zones with their associated seismicity for: a) top 50 km and b) 50 to 700 km depth. ACR: 1) Australian Plate; 2) Pacific Plate; 3) Tonga Ridge (North); 4) Lau Basin; 5) Fonualei discontinuity; 10) Tonga Ridge-A; 11) Tonga Ridge-B; SZ: 6) Tonga Interplate-B; 7) Intraslab intermediate (50-410 km); 8) Intraslab deep (410-700 km); 9) Tonga Interplate-A.

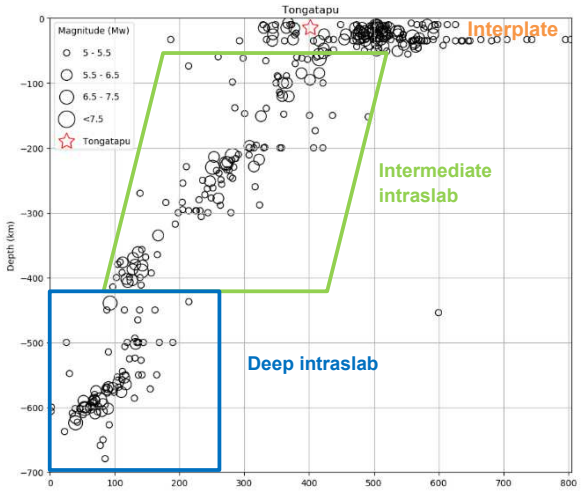

Figure 5. Cross section across Tongatapu, transverse to the Tonga Trench with associated seismicity. Red star indicates location of Tongatapu.

4.1 *Source parameters*

All sources were modelled using the Guttenberg-Richter (G-R) doubly truncated exponential magnitude distribution. The minimum magnitude (M_{min}) was set at M_w=5.0. The maximum magnitude (M_{max}) was estimated by increasing by 0.5 units the maximum observed earthquake magnitude of each source, known to be not ideal and conservative assumption in practice. Empirical and statistical models available for this were not possible to implement given the limited knowledge from characteristics of the tectonic features from each source.

Linear regression was used to estimate the activity rate and the slope of the recurrence equation for most source zones, except for zones 1, 3, 5 and 10, where Bayesian regression was employed, to increase statistical quality of data in zones with lower seismic activity. In the Bayesian regression the posterior

distribution of the mean was set as prior knowledge. The main recurrence parameters are listed in Table 1 and Figure 6 illustrates the G-R occurrence rates for the complete catalog.

Table 1. Summary of the recurrence parameters. *a* and *b*: constants from the regressions; $v_{5.0}$: number of earthquakes per year with magnitude larger than M_{min}; β: *b Ln(10)*; M_{max}: maximum magnitude; $M_{max(obs)}$: maximum observed magnitude

Source zone	*Nr. events*	*a*	$v_{5.0}$	*b*	β	$M_{max\ (obs)}$	M_{max}
All	2863	3.65	44.88	1.07	2.47	8.15[b]	8.65
1	50	1.64[a]	0.63	1.16[a]	2.67	6.12[c]	6.62
2	330	2.45	2.84	0.89	2.05	8.10[c]	8.60
3	40	1.57[a]	0.54	1.15[a]	2.64	6.14[c]	6.64
4	105	2.38	2.37	1.17	2.69	6.86[b]	7.36
5	41	1.56[a]	0.53	1.13[a]	2.60	6.34[c]	6.84
6	578	3.29	19.50	1.36	3.14	7.50[c]	8.00
7	994	3.10	12.64	1.01	2.32	8.04[b]	8.54
8	417	2.80	6.25	0.96	2.21	8.15[b]	8.65
9	151	2.51	3.23	1.19	2.75	7.39[c]	7.89
10	36	1.47[a]	0.43	1.11[a]	2.56	6.33[c]	6.83
11	121	2.09	1.22	0.86	1.99	7.97[c]	8.47

[a]Bayesian regression; [b]ISC (2019); [c]ISC-GEM (2019).

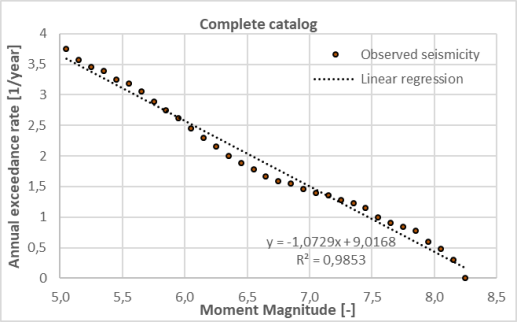

Figure 6. G-R occurrence rates for exponential model for the complete catalog.

4.2 *Ground motion prediction equations (GMPE)*

There are no GMPE's specific for the region. Regional GMPE's available from literature and the previous regional PSHA (Rong et al., 2010, 2012; Petersen et al., 2012) were reviewed to select appropriate GMPE's for each tectonic regime (ACR and SZ in this case). To prevent subjectivity and to ensure quality of the analysis, the exclusion criteria from Cotton et al. (2006), Bommer et al., (2010) and Stewart et al. (2015) were followed.

Four GMPEs were selected for ACR from the NGA-West 2 project: Boore et al. (2014), BEA14; Abrahamson et al. (2014), ASK14; Campbell and Bozorgnia (2014), CB14; and Chiou and Youngs (2014), CY14. These GMPEs represent the latest developments in global attenuation models with extended databases, reviewed functional forms and wider ranges in magnitudes (Boore et al., 2014). For SZ four GMPEs were chosen: Youngs et al. (1997), YEA97; Atkinson and Boore (2003), AB03; Zhao et al. (2006), ZEA06; and Abrahamson et al. (2016), AEA16.

4.3 *Logic tree and uncertainties*

The selected GMPEs were equally weighted with a logic tree framework to account for epistemic uncertainties from the ground motion models, as illustrated in Figure 7. Other epistemic uncertainties, for instance M_{max} or areal definition of the seismogenic sources were covered after some sensitivity assessments, implementing conservative assumptions.

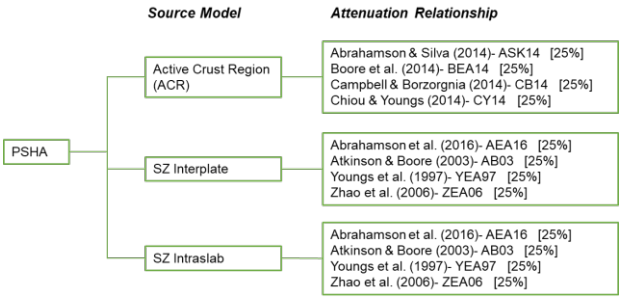

Figure 7. Logic tree used for the hazard calculation.

5 PSHA RESULTS

The hazard calculations were executed in R-CRISIS (v.18.4.2, 2019) for two site conditions with Vs30 of 760m/s and 400m/s and four scenarios: 50%, 10%, 5% and 2% probability of exceedance in 50 years.

5.1 *Hazard curves and uniform spectra*

The probabilistic analysis included ground motion measures for different spectral accelerations at different oscillator periods, up to 3 seconds, given the restrictions from some GMPE's (Figure 8). For reasons of space, only the hazard curves related to PGA are shown in Figure 9 and summarized in Table 2.

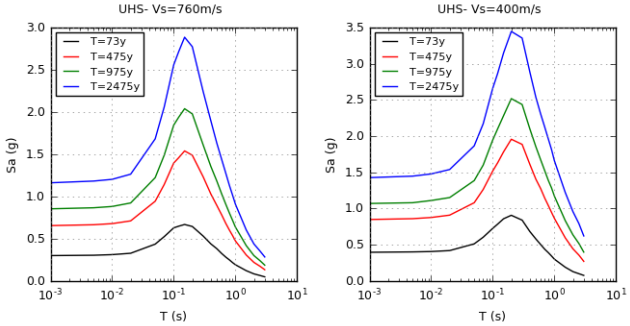

Figure 8. Mean UHS with 5% damping for sites with V_{s30} of 760 m/s (left) and 400 m/s (right).

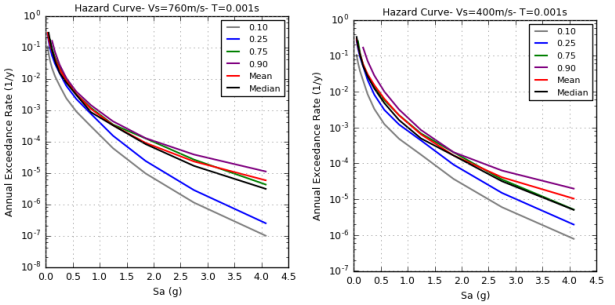

Figure 9. Hazard curves for PGA for sites with V_{s30} of 760 m/s (left) and 400 m/s (right) for different centiles and mean results.

Table 2. Spectral acceleration (Sa) in [g] per return period (Tr in years)

V_{s30} [m/s]	Sa	Tr=73	Tr=475	Tr= 975	Tr=2475
760	PGA	0.30	0.66	0.85	1.16
	0.2	0.64	1.49	1.98	2.77
	1.0	0.19	0.47	0.64	0.91
400	PGA	0.40	0.85	1.07	1.43
	0.2	0.91	1.96	2.52	3.44
	1.0	0.30	0.86	1.17	1.66

5.2 *Hazard disaggregation*

Seismic source disaggregation is used to understand which source(s) contributes more to the hazard at a given hazard scenario, in terms of return period, ground condition, spectral acceleration. The hazard was disaggregated in terms of magnitude, distance and epsilon combinations, as shown in Figure 10. Linear bin spacing was used with bin widths of 0.5 and 25km for magnitude and distance, respectively.

The disaggregation results were obtained for each branch of the logic tree for two return periods (475 and 2475 years). For illustration, example plots are shown in Figure 10. For the 475 years return period, the hazard-dominating scenario obtained from all the disaggregations, comprises large magnitude (M_w 7.5-8.0) at short epicentral distance (25–50km), associated to the activity from the Tonga Ridge B (source zone 11, Figure 4). The disaggregation results obtained from the different branches of the logic tree and qualitatively compatible, despite the complexity introduced when two GMPEs representing different tectonic environments are combined in one branch. For the 2475y return period two trends were found governing hazard: one main source at 50-75km with associated magnitude M_w 8.25-8.5 and a main source at 25-50km with associated magnitude M_w 7.75-8.0. The sources associated to these outcomes would be likely the Tonga Ridge B and/or Tonga interplate or Intranslab intermediate (zones 11, 6 or 7, Figure 4).

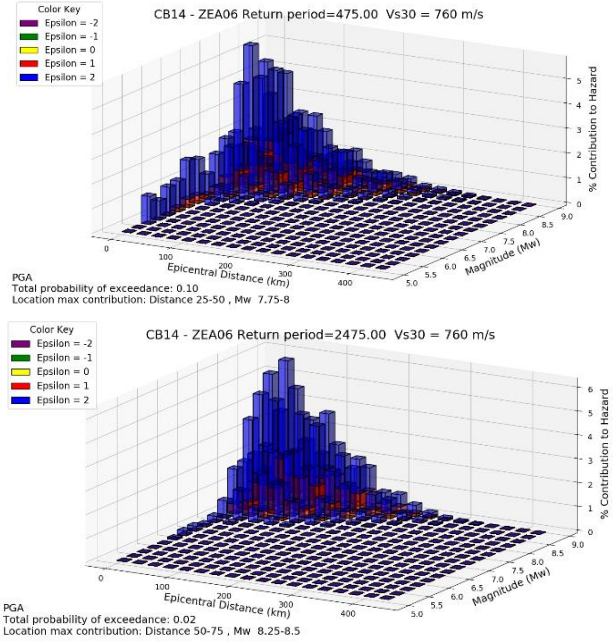

Figure 10. Example disaggregated hazard for PGA for 475 and 2475 years return periods using CB14 and ZEA16 GMPE's and V_{S30}=760m/s ground condition.

6 CONCLUSIONS

The site-specific PSHA executed for Nuku'alofa Port is the result from a comprehensive effort covering the available hazard knowledge in the region and best available input data and methods to set the analysis. The findings demonstrate a high seismic hazard. The main findings are summarized as:

- The hazard outcomes from this work have higher PGA than the probabilistic models from Rong et al. (2012). Rong's work only shows PGA for the 475 years return period, having a 0.49g, while this study obtained a 0.66g PGA for the same scenario. On the other hand, the outcomes from this work are somewhat lower but closer to the outcomes from Petersen et al. (2012). The seismic sources interpreted for this work are similar to Rong's and include crustal active sources, whereas Petersen's did not. Differences might be related to the completeness times and subsequent recurrence parameters interpretation. The GMPE's used in this work are not fully aligned to the previous studies but are newer improved versions from ones used in Rong's and Petersen's works.
- The magnitude-distance disaggregation indicates a major contribution to the hazard from the near-source (25-50km) Tonga Ridge B (zone 11, Figure 4) for all the return periods.

The findings from this study are site-specific and applicable only for Nuku'alofa and the specified ground conditions and scenarios.

7 ACKNOWLEDGEMENTS

This work was part of the Climate and Disaster Risk Assessment executed within the Nuku'alofa Port Upgrade project funded by the Asian Development Bank (ADB). The authors acknowledge Royal HaskoningDHV and ADB for the opportunity.

8 REFERENCES

Abrahamson, N., Gregor, N., and Addo, K. 2016. BC Hydro ground motion prediction equations for subduction earthquakes, *Earthquake Spectra* 32(1), 23–44.

Abrahamson, N., Silva, W., and Kamai, R. 2014. Summary of the ASK14 Ground-Motion Relation for Active Crustal Regions. *Earthquake Spectra* 30(3), 1025-1055.

Atkinson, G.M., and Boore, D.M. 2003. Empirical Ground-Motion Relations for Subduction-Zone Earthquakes and Their Application to Cascadia and Other Regions. *Bulletin of the Seismological Society of America* 93(4), 1703-1729.

Austin, J.A., Taylor, F.W., 1989. Seismic stratigraphy of the Central Tonga Ridge. *Marine and Petroleum Geology* 6(1), 71-92.

Bevis, M., Taylor, F. W., Schutz, B. E., Recy, J., Isacks, B. L., Helu, S., Singh, R., Kendrick, E., Stowell, J., Taylor, B. and Calmant, S., 1995. Geodetic observations of very rapid convergence and back-arc extension at the Tonga arc. *Nature* 374, 249-251.

Bommer, J. Douglas, J., Scherbaum, F., Cotton, F., and Bungum, H. 2010. On the selection of ground-motion prediction equations for seismic hazard analysis. *Seismological Research Letters* 81(5), 783-793.

Boore, D.M., Stewart, J.P., Seyhan, E., and Atkinson, G.M. 2014. NGA-West2 Equations for Predicting PGA, PGV, and 5% Damped PSA for Shallow Crustal Earthquakes. *Earthquake Spectra* 30(3), 1057-1085.

Bormann, P., and Saul, J. 2008. The new IASPEI standard broadband magnitude m(B). *Seismological Research Letters* 79, 698-705. 10.1785/gssrl.79.5.698.

Campbell, K.W., and Boorgnia, Y. 2014. NGA-West2 Ground Motion Model for the Average Horizontal Components of PGA, PGV, and 5% Damped Linear Acceleration Response Spectra. *Earthquake Spectra* 30(3), 1087-1115.

Chiou, B.S.-J., and Youngs, R.R. 2014. Update of the Chiou and Youngs NGA Model for the Average Horizontal Component of Peak Ground Motion and Response Spectra. *Earthquake Spectra* 30(3), 1117-1153.

Cotton, F., Scherbaum, F., Bommer, J., and Bungum, H. 2006. Criteria for selecting and adjusting ground-motion models for specific target regions: Application to Central Europe and rock sites. *Journal of Seismology* 10(2), 137-156.

Di Giacomo, D., E.R. Engdahl, and D.A. Storchak 2018. The ISC-GEM Earthquake Catalogue (1904–2014): status after the Extension Project. *Earth System Science Data* 10, 1877-1899, doi: 10.5194/essd-10-1877-2018.

Di Giacomo, D., I. Bondár, D.A. Storchak, E.R. Engdahl, P. Bormann, and J. Harris 2015. ISC-GEM: Global Instrumental Earthquake Catalogue (1900-2009): III. Re-computed MS and mb, proxy MW, final magnitude composition and completeness assessment. *Physics of the Earth and Planetary Interiors* 239, 33-47, doi: 10.1016/j.pepi.2014.06.005.

Geoscience Australia 2019. Earthquakes@GA. *Australian Government*, https://earthquakes.ga.gov.au/

ISC 2019. On-line Bulletin. https://doi.org/10.31905/D808B830

ISC-GEM 2019. ISC-GEM Global Instrumental Earthquake Catalog. https://doi.org/10.31905/d808b825

McGuire, R.K. 2004. Seismic hazard and risk analysis. *Earthquake Engineering Research Institute,* MNO-10, Boulder-Colorado, 221p.

Pagani, M., Garcia-Pelaez, J., Gee, R., Johnson, K., Poggi, V., Styron, R., Weatherill, G., Simionato, M., Viganò, D., Danciu, L., and Monelli, D. 2018. Global Earthquake Model (GEM) Seismic Hazard Map (version 2018.1 - December 2018), DOI: 10.13117/GEM-GLOBAL-SEISMIC-HAZARD-MAP-2018.1 [12/03/2019]

Petersen, M.D., Harmsen, S.C., Rukstales, K.S., Mueller, C.S., McNamara, D.E., Luco, N., and Walling, M. 2012. Seismic hazard of American Samoa and neighboring South Pacific Islands – Data, Methods, Parameters and Results. *USGS Open-File Report* 2012-1087, https://pubs.usgs.gov/of/2012/1087/OF12-1087.pdf

R-CRISIS 2019. Validation and Verification Document. *Program for Probabilistic Seismic Hazard Analysis*, Mexico City, 290 p.

Rong, Y., Mahdyiar, M., Shen-Tu, B., Shabestari, K.T., and Guin, J. 2010. Probabilistic seismic hazard assessment for South Pacific Islands. *Proceeding of 9th US National Conference on Earthquake Engineering (9NCEE)*, 25-29, July 2010.

Rong, Y., Park, J., Duggan, D., Mahdyiar, M., and Bazzurro, P. 2012. Probabilistic Seismic Hazard Assessment for Pacific Island Countries. *Proceedings of 15th World Conference on Earthquake Engineering*. Lisbon, Portugal: ISBN: 978-1-63439-651-6. https://doi.org/10.13140/2.1.4301.0568.

SED 2016. Global seismic hazard (GSHAP). Retrieved from Global seismic hazard (GSHAP): http://map.seismo.ethz.ch/map-apps/map-viewer/index.html

Spennemann, D. H., 1997. A Holocene sea-level history for Tongatapu, Kingdom of Tonga. Coastal and Environmental geoscience studies of the Southwest Pacific Islands. *SOPA Technical Bulletin* 9, 115-152.

Stewart, J.P., Douglas, J., Javanbarg, M., Abrahamson, N.A., Bozorgnia, Y., Boore, D.M., Campbell, K.W., Delavaud, E., Erdik, M., and Stafford, P.J. 2015. Selection of ground motion prediction equations for the Global Earthquake Model. *Earthquake Spectra* 31(1), 19-45.

USGS 2019. Search Earthquake Catalog. *Earthquake Hazards Program*, https://earthquake.usgs.gov/earthquakes/search/

Wells D.L., and Coppersmith K.J. 1994. New empirical relationships among magnitude, rupture length, rupture width, rupture area and surface displacement. *Bulletin of the Seismological Society of America* 84(4), 974-1002.

Youngs, R.R., Chiou, S.-J., Silva, W.J., and Humphrey, J.R. 1997. Strong ground motion attenuation relationships for subduction zone earthquakes. *Seismological Research Letters* 68(1), 58-73.

Zhao, J.X., Zhang, J., Asano, A., Ohno, Y., Oouchi, T., Takahashi, T., Ogawa, H., Irikura, K., Thio, H.K., Somerville, P.G., Fukushima, Y., and Fukushima, Y. 2006. Attenuation relations of strong motion in Japan using site classification based on predominant period. *Bulletin of the Seismological Society of America* 96(3), 898-913.